

1 **Optimization of the hydrolysis of lignocellulosic**  
2 **residues by using radial basis functions modelling and**  
3 **particle swarm optimization**

4

5

6 Pablo C. Giordano<sup>a,b</sup>, Alejandro J. Beccaria<sup>b</sup>, Héctor C. Goicoechea<sup>a,\*</sup> and Alejandro C.  
7 Olivieri<sup>c,\*</sup>

8

9

10 <sup>a</sup> *Laboratorio de Desarrollo Analítico y Quimiometría (LADAQ), Cátedra de Química*  
11 *Analítica I, Facultad de Bioquímica y Ciencias Biológicas, Universidad Nacional del*  
12 *Litoral, Ciudad Universitaria, CC 242 (S3000ZAA), Santa Fe, Argentina.*

13 <sup>b</sup> *Laboratorio de Fermentaciones, Facultad de Bioquímica y Ciencias Biológicas,*  
14 *Universidad Nacional del Litoral, Ciudad Universitaria, CC 242 (S3000ZAA), Santa*  
15 *Fe, Argentina.*

16 <sup>c</sup> *Departamento de Química Analítica, Facultad de Ciencias Bioquímicas y*  
17 *Farmacéuticas, Universidad Nacional de Rosario, Instituto de Química de Rosario*  
18 *(IQUIR-CONICET), Suipacha 531, Rosario, S2002LRK, Argentina.*

19

20

21

---

\* Corresponding authors. E-mail addresses: [olivieri@iquirconicet.gov.ar](mailto:olivieri@iquirconicet.gov.ar) (A.C. Olivieri) and [hgoico@fcb.unl.edu.ar](mailto:hgoico@fcb.unl.edu.ar) (H.C. Goicoechea).

22 **Abstract**

23 The concentrations of glucose and total reducing sugars obtained by chemical  
24 hydrolysis of three different lignocellulosic feedstocks were maximized. Two response  
25 surface methodologies were applied to model the amount of sugars produced: (1)  
26 classical quadratic least-squares fit (QLS), and (2) artificial neural networks based on  
27 radial basis functions (RBF). The results obtained by applying RBF were more reliable  
28 and better statistical parameters were obtained. Depending on the type of biomass,  
29 different results were obtained. Improvements in fit between 35 % and 55 % were  
30 obtained when comparing the coefficients of determination ( $R^2$ ) computed for both QLS  
31 and RBF methods. Coupling the obtained RBF models with particle swarm optimization  
32 to calculate the global desirability function, allowed to perform multiple response  
33 optimization. The predicted optimal conditions were confirmed by carrying out  
34 independent experiments.

35

36 **Keywords:** Glucose, Modelling, Optimization, Artificial Intelligence, Particle swarm  
37 optimization, Radial basis functions.

38

39

## 40 **1. Introduction**

41 Experimentalists have several techniques available for finding optimal process  
42 conditions. These approaches vary from the traditional one-variable-at-a-time method to  
43 more complex statistical and mathematical techniques involving experimental designs,  
44 such as full and fractional factorial, and central composite designs, followed by  
45 optimization techniques such as the response surface methodology (RSM) [1].

46 Experimental design and RSM have been proved to be useful for developing,  
47 improving and optimizing processes, and have been extensively used in the industrial  
48 world [2–9] and in bioprocesses [10–16], including the formulation of culture media for  
49 bacteria and fungi [17–20].

50 When RSM is applied, the experimental responses are usually fitted to quadratic  
51 functions by least-squares (QLS). In most of the cases which have been studied by this  
52 methodology, a second-degree polynomic relation can reasonably approximate the  
53 behavior of the systems under study.

54 Artificial neural networks (ANN) represent another smart tool for non-linear  
55 multivariate modeling. The power of an ANN lies in its universal structure and in its  
56 ability to learn from historical data. Among the main advantages of ANN compared to  
57 QLS, the former do not require a prior specification of a suitable fitting function and  
58 have universal approximation capability, i.e. they can approximate almost all kinds of  
59 non-linear functions, including quadratic functions. QLS, on the other hand, is only  
60 useful for quadratic approximations; it should be noticed that more complex functions  
61 require a larger number of experiments [21]. QLS and ANN have been applied in  
62 diverse areas such as in the vehiculization of therapeutic drugs [22], and in the  
63 production of recombinant proteins [23,24,25], bioinsecticides [26], biopolymer  
64 scleroglucan [21], and endonuclease derived from recombinant *Esheria coli* [27].

65 Artificial neural networks based on the use of radial basis functions (RBF) have  
66 been recently introduced for nonlinear multivariate function estimation and regression  
67 tasks [28]. RBF networks have a single hidden layer of neurons incorporating gaussian  
68 transfer functions, and a linearly activated output layer. In comparison with multi-layer  
69 perceptron (MLP) networks, RBF offer some advantages such as robustness towards  
70 noisy data as well as a faster training phase [29].

71 In the context of regression analysis, recent RBF publications which deserve to be  
72 cited describe applications to near-infrared analysis of organic matter in soils [30],  
73 glucose in blood [31], and water content in fish products [32]. In the field of  
74 optimization, RBF was used for the prediction of optimal culture conditions for  
75 maximum hairy root biomass yield [33].

76 In the present report, the RBF modeling power is complemented with a stochastic  
77 procedure for finding global minima called particle swarm optimization (PSO). This  
78 latter technique has been shown to successfully optimize a wide range of continuous  
79 functions [34], based on concepts loosely related to social interaction issues. It searches  
80 a space by adjusting the trajectories of individual vectors, called “particles”, while they  
81 move in a multidimensional space. The individual particles are drawn stochastically  
82 toward the positions of their own previous best performance and the best previous  
83 performance of their neighbours [35].

84 The combination RBF-PSO, which has been successfully applied by Liu et al. [36]  
85 and Kitayama et al. [37], is herein applied to optimize the conditions for the chemical  
86 hydrolysis of lignocellulosic feedstocks (corn bran, wheat bran and pine sawdust). The  
87 results show that the conditions reached by RBF-PSO are much more realistic than  
88 those obtained from QLS.

89

90 **2. Materials and methods**

91 *2.1. Raw materials*

92 Corn bran, wheat bran and pine sawdust were gently provided by Marchisio-  
93 Fernandez SRL, Santa Fe, Argentina. Each feedstock was air-dried, milled,  
94 homogenized in a single lot and stored under dry conditions before use. The feedstocks  
95 were milled in a Wiley knife mill (Standard Model No. 3, Arthur H. Thomas,  
96 Philadelphia, USA) to pass through a 1.0 mm screen. In a further step, the milled  
97 feedstocks were passed through a 0.5 mm sieve, thus obtaining 2 batches for each  
98 feedstock (one containing particles between 0.5 mm and 1.0 mm and the other one,  
99 particles with a size less than 0.5 mm).

100

101 *2.2 Hydrolysis process*

102 Feedstocks were chemically hydrolyzed using solutions of sulphuric acid. In each  
103 experiment, the mass of feedstock was mixed with the acid solution in 15 mL closed  
104 polypropilene tubes. Each mixture was incubated at different temperatures and during  
105 different periods of time, according to the central composite designs (CCD) employed  
106 in this study. The incubation was performed by dipping the tubes in a water bath. After  
107 the time of hydrolysis was complete, the liquid fraction was recovered by centrifugation  
108 at 5000 rpm for 10 minutes plus further filtration with filter paper. All liquid fractions  
109 recovered were stored at  $-18\text{ }^{\circ}\text{C}$  until sugars quantitation. A control assay was made  
110 using filter paper to take into account any contribution of this material to sugars  
111 concentration that could occur in the filtration step.

112

113 *2.3 Central composite design and RBF-PSO approach*

114 A CCD was introduced in this study to optimize the chemical hydrolysis process of  
115 three different feedstocks. According to this design, each variable was examined at five  
116 levels:  $-\alpha$ ,  $-1$ ,  $0$ ,  $+1$  and  $+\alpha$ .

117 Since the application of QLS was not successful in achieving the modeling of the  
118 hydrolysis processes, an RBF-PSO approach was used to obtain the optimal factor  
119 levels that guarantee the maximization of the responses. In the present work, an RBF  
120 network combined with forward selection was used, and for PSO, the population size  
121 and the number of generations were estimated by trial and error, set as fifteen particles  
122 (wheat bran) or ten particles (corn bran and pine sawdust) and fifteen generations in  
123 both cases. The value of the global desirability function (D) was the objective function  
124 to be optimized [38].

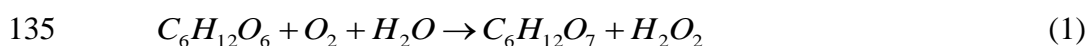
125 In the present work, three or four factors were varied in order to obtain the optimal  
126 conditions for the chemical hydrolysis of pine sawdust, corn bran and wheat bran.

127

#### 128 *2.4 Analytical method*

129 The glucose concentration was enzymatically measured by using a commercial kit  
130 (Wiener Lab, Argentina). This quantitation method consists of two steps: first,  
131 according to Eq. (1), the glucose oxidase catalyzes the oxidation reaction of glucose to  
132 gluconic acid, with the consequent consumption of oxygen and water, and the  
133 generation of hydrogen peroxide.

134

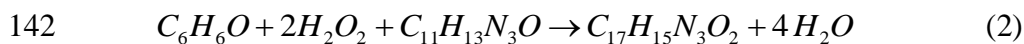


136

137 In the second step, according to Eq. (2), a peroxidase catalyzes the reaction  
138 between two molecules of hydrogen peroxide with phenol and 4-aminophenazone to

139 generate four molecules of water and a colored compound known as 4-(p-  
140 benzoquinone monoimine)-phenazone, which has an absorption maximum at 505 nm.

141



143 The concentration of reducing sugars was measured by using a well-known  
144 chemical method [39].

145

## 146 2.5. Software

147 All the collected data were transferred to a PC Intel Celeron D for their further  
148 interpretation. Design Expert™ version 8.05.0 (Stat-Ease, Inc, Minneapolis, USA,  
149 2010) was used to perform experimental design.

150 RBF networks were implemented using the forward selection method described by  
151 Orr in ref [40] and available at <http://www.anc.ed.ac.uk/rbf/rbf.html>. The complete  
152 RBF-PSO optimization algorithm was written in MATLAB R2008a (The MathWorks,  
153 Inc.).

154

## 155 3. Theory

### 156 3.1. Radial basis function networks

157 Artificial neural networks based on radial basis functions consist of three layers. The  
158 neurons of the input layer distribute the input variables (which in our case are the  $F$   
159 factor values influencing a given response) to the neurons of the hidden layer. Each of  
160 the  $M$  neurons of the hidden layer transfers the input data through a Gaussian function  
161 to the output layer. Finally, the output neuron uses a linear transfer function, in contrast  
162 to MLP networks, which employ non-linear transfer functions. To specifically  
163 implement RBF networks, suitable parameters for the Gaussian functions of the hidden

164 layer are needed. They consist of the centres of the Gaussian functions (contained in the  
 165  $F \times 1$  vector  $\mathbf{c}_m$ ) and the Gaussian widths  $\sigma$ , which are typically taken as identical for all  
 166 functions. The output value from the  $m$ th. hidden neuron for a given input value  $\mathbf{x}_i$ , is  
 167 thus given by:

$$168 \quad \text{out}_m = \exp\left(-\frac{1}{2\sigma^2} \|\mathbf{x}_i - \mathbf{c}_m\|^2\right) \quad (3)$$

169 where  $\|\mathbf{x}_i - \mathbf{c}_m\|$  is the length of the vector difference and equal to the distance between  
 170  $\mathbf{x}_i$  and  $\mathbf{c}_m$ . The input value to the output node is the weighted sum of all the outputs of  
 171 the hidden nodes. Finally, the response of the output node is linearly related to its input.  
 172 Therefore, the RBF network output ( $\text{out}_i$ ) for an input object  $\mathbf{x}_i$  can be written as:

$$173 \quad \text{out}_i = w_0 + \sum_{m=1}^M w_m \exp\left(-\frac{1}{2\sigma^2} \|\mathbf{x}_i - \mathbf{c}_m\|^2\right) \quad (4)$$

174 where  $w_0$  is the so-called bias, and  $w_m$  is the weight ascribed to the  $m$ th. hidden output.  
 175 The weights are adjusted so that the mean square error of the net output (with regard to  
 176 reference values) is minimized. The parameters to be adjusted are the Gaussian centres  
 177 and widths of the hidden neurons, and the weights of the output layer. The RBF  
 178 networks show a guaranteed convergence in their learning procedure: from the centres  
 179 of the  $M$  basis functions and a set of  $I$  training objects with known factor values ( $\mathbf{x}_i$ ) and  
 180 target response ( $r_i$ ), the minimum squared error in the prediction of  $r$  can be shown to be  
 181 lead to the following weights:

$$182 \quad \mathbf{w} = (\mathbf{H}^T \mathbf{H})^{-1} \mathbf{H}^T \mathbf{r} \quad (5)$$

183 where  $\mathbf{w}$  ( $M \times 1$ ) collects the weights,  $\mathbf{r}$  ( $I \times 1$ ) the target response values, and  $\mathbf{H}$  ( $I \times M$ ) is  
 184 the design matrix whose elements are:

$$185 \quad H(i, m) = \exp\left(-\frac{1}{2\sigma^2} \|\mathbf{x}_i - \mathbf{c}_m\|^2\right) \quad (6)$$



186 Several procedures exist to limit the dimensionality of the hidden layer. One  
187 alternative is to control the network complexity using a subset of possible centres,  
188 which can be found by forward selection. The latter starts with an empty model and  
189 adds new functions, centred on each data point, according to the degree in which these  
190 functions reduce the squared error. Orr [41] combined forward selection with  
191 regularization involving the additional parameter  $\lambda$  in Eq. (5), to penalize for large  
192 weight values:

$$193 \quad \mathbf{w} = (\mathbf{H}^T \mathbf{H} + \lambda \mathbf{I})^{-1} \mathbf{H}^T \mathbf{y} \quad (7)$$

194 where  $\mathbf{I}$  is an appropriately dimensioned unit matrix. Our specific RBF working  
195 parameters are provided below.

196 It may be noticed that RBF are different from MLP networks in the following  
197 aspects: 1) RBF networks have a single hidden layer, whereas MLP may have several,  
198 2) the hidden (non-linear) RBF layer is different from output (linear) layer, while in  
199 MLP there is a common neuronal model for all layers and 3) the argument of the RBF  
200 transfer function is the Euclidean distance between the input vector and the centre,  
201 while MLP compute the inner product of the input vector and the synaptic weight  
202 vector.

203

### 204 *3.2. Particle swarm optimization*

205 Particle swarm optimization is a technique inspired in a natural process, in this case  
206 the collective motion of birds. In PSO, a number of particles is given initial random  
207 positions and velocities, and the positions allow to evaluate a certain objective function.  
208 In the present case, the positions are the factors, defined in a space having a number of  
209 dimensions equal to the number of factors  $F$ , while the objective function to be  
210 minimized is the sum of squared errors SSE (predicted vs. measured response). Both the

211 particle positions and velocities are subsequently tuned employing well-defined rules,  
 212 with the new positions allowing one to evaluate new function values in each running  
 213 cycle. Whenever a particle finds a position which is better than those previously found  
 214 (because the SSE is lower), its coordinates are stored. The new position of each particle  
 215 is then defined within the context of a neighbourhood which comprise the particle itself  
 216 and other particles in the population. This is achieved by defining the velocity in future  
 217 time steps as a linear combination of: (1) the current velocity, (2) the difference between  
 218 the overall best position and the actual individual position and (3) the stochastically  
 219 weighted difference between the neighbourhood best position and the individual current  
 220 position:

$$221 \quad v_{ia,t+1} = w(t)v_{ia,t} + c_1(p_{ia,t} - x_{ia,t}) + c_2(p_{a,t} - x_{ia,t}) \quad (8)$$

222 where  $v_{ia,t}$  and  $v_{ia,t+1}$  are the velocities for the  $i$ th. particle in the  $a$ th. dimension at times  $t$   
 223 and  $t+1$  respectively,  $x_{ia,t}$  is its current position,  $p_{ia,t}$  is its best position,  $p_{a,t}$  is the best  
 224 position for any member of the population,  $w(t)$  is a time-dependent weight, and  $c_1$  and  
 225  $c_2$  are adjustable parameters. The weight  $w(t)$  decreases with time to ensure that position  
 226 changes in the last cycles monotonically decrease:

$$227 \quad w(t) = w_0 + \frac{w_\infty - w_0}{t_{\max}} t \quad (9)$$

228 where  $w_0$  and  $w_\infty$  ( $w_0 > w_\infty$ ) are adjustable parameters, and  $t_{\max}$  is the maximum number  
 229 of time cycles. Usually the value provided by equation (8) is compared with a certain  
 230 maximum velocity  $v_{\max,a}$  and the least of them is added to the particle position:

$$231 \quad x_{ia,t+1} = x_{ia,t} + |v_{ia,t+1}| \times \min(|v_{ia,t+1}|, v_{\max,a}) / v_{ia,t+1} \quad (10)$$

232 where  $|\cdot|$  implies the modulus. These rules for particle movement cause them to search  
 233 between two best positions: the individually best point and the globally best one, in a  
 234 manner which is related to some social activities such as bird flocking. Figure 1 shows

235 the flow sheet for the PSO scheme employed in this study. Specific details concerning  
 236 the PSO process are provided below.

237

### 238 3.3. Desirability function

239 The use of a desirability function involves creating a function for each individual  
 240 response  $d_i$  and finally obtaining a global function  $D$  that should be maximized choosing  
 241 the best conditions of the designed variables. The latter function varies from 0 (value  
 242 totally undesirable) to 1 (all responses are in a desirable range simultaneously), and can  
 243 be defined by Eq. (17):

$$244 \quad D = \left( d_1^{r_1} \times d_2^{r_2} \right)^{\frac{1}{r_1+r_2}} \quad (11)$$

245 where  $d_1$  and  $d_2$  correspond to the individual desirability functions for the responses  
 246 being optimized, and  $r_1$  and  $r_2$  measure the relative importance of each response. In the  
 247 present report, both responses were assigned the same importance, i.e.,  $r_1 = r_2 = 1$ .

248 Individual desirabilities ( $d_1$  and  $d_2$ ) were computed with the following maximization  
 249 function:

$$250 \quad d_i = \begin{cases} \left( \frac{\hat{Y} - A}{B - A} \right)^{w_i} & , \quad A \leq \hat{Y} \leq B \\ 1 & , \quad \hat{Y} > B \\ 0 & , \quad \hat{Y} < A \end{cases} \quad (12)$$

251 where  $A$  and  $B$  correspond to the lower and maximum limit, respectively (see values in  
 252 Table 5),  $\hat{Y}$  is the predicted response (by the RBF model), and  $w_i$  the weights (if a  
 253 weight is 1, the  $d_i$  values will vary from 0 to 1 in a linear way while approaching to the  
 254 desired value). In the present report, weights were both set to 1.

255

256

#### 257 **4. Results and discussion**

258 With the aim of optimizing the chemical hydrolysis processes of three feedstocks  
259 (corn bran, wheat bran and pine sawdust), three CCDs were built (one for each  
260 feedstock). Two of them, corresponding to corn bran and pine sawdust, consisted of  
261 twenty experiments: six center, six axial and eight factorial points. On the other hand,  
262 the one corresponding to wheat bran consisted of thirty experiences: six center, eight  
263 axial and sixteen factorial points. The independent variables taken into account to build  
264 the experimental designs were previously selected by building Plackett-Burman designs  
265 and applying a GA approach [42]. Additional variables, i.e. particle size, pretreatment  
266 and time of hydrolysis (in corn bran and pine sawdust cases), which were not found to  
267 be significant, were kept constant.

268 In the case of corn bran and pine sawdust, the three evaluated factors were: (1)  
269 temperature of hydrolysis ( $T_e$ ), (2) sulfuric acid concentration ( $A$ ), and (3) acid  
270 solution/feedstock ratio ( $AF$ ). In the wheat bran case, four factors were evaluated: the  
271 latter three and also the time of hydrolysis ( $T_i$ ). Additionally, none of the feedstocks  
272 were chemically pretreated, and the feedstock particle sizes employed were: 1.0 mm for  
273 corn bran and 0.5 mm for both wheat bran and pine sawdust.

274 A literature search revealed that the sugars/raw biomass yield is usually employed  
275 as a response to be optimized, because it is assumed to be a better descriptor of the  
276 hydrolysis process. However, Vieira Canettieri et al. [43] suggested that the  
277 polysaccharide content (hemicellulose and cellulose) of the raw biomass should also be  
278 taken into account, in order to calculate an “extraction percentage”, since a good yield  
279 does not guarantee a good conversion from polysaccharides to monosaccharides.  
280 Because the aim of this study was to obtain as much monosaccharides as possible, it  
281 was decided that for the three evaluated feedstocks, the two responses to be measured

282 are the concentrations (in  $\text{g L}^{-1}$ ) of glucose (G) and reducing sugars (RS). Table 1 and 2  
283 summarize the twenty and thirty experiments, and the concentrations of G and RS  
284 obtained for corn bran, pine sawdust and wheat bran, respectively.

285 Since the application of response surface methodology with quadratic least-squares  
286 through a CCD was not successful in obtaining the optimal hydrolysis conditions for  
287 each feedstock (see below), a different optimization procedure, based on RBF networks  
288 coupled to PSO, was applied to achieve this objective. By employing an RBF network,  
289 the multidimensional space was adequately modeled. Then, in a subsequent step, by  
290 applying a PSO approach, the modelled multidimensional space was screened, and the  
291 optimal hydrolysis conditions for each one of the three feedstocks were obtained, with  
292 the corresponding value of desirability D.

293 Finally, a comparison of the determination coefficients ( $R^2$ ) corresponding to both  
294 models was carried out, in order to verify that the models obtained by RBF networks  
295 were better than those yielded by the application of QLS.

296

#### 297 *4.1 Analysis by quadratic least-squares*

298 The ANOVA tests applied to the factors and responses data demonstrated that six  
299 quadratic models could fit both G and RS responses for the three feedstocks under  
300 consideration. The associated probability values ( $p$ ) obtained for the G response models  
301 were  $7 \times 10^{-4}$ ,  $9 \times 10^{-4}$  and  $1 \times 10^{-2}$  for wheat bran, corn bran and pine sawdust,  
302 respectively, while the corresponding  $p$  values for the RS response models were  $1 \times 10^{-4}$   
303 for the three cases, thus indicating the significance of the models, which can be  
304 mathematically expressed according to Equations (13) to (18).

305

306 For wheat bran:

307  $Y_1 = -41.812.69X_3 - 10.49X_4 - 0.11X_1X_4 - 0.04X_2X_3 + 0.75X_4^2$  (13)

308  $Y_2 = -383.21 + 7.39X_2 + 12.56X_3 - 1.14X_4 - 0.04X_1X_3 - 0.06X_2X_3$   
 $- 0.11X_2X_4 - 0.03X_2^2 - 0.12X_3^2 + 0.30X_4^2$  (14)

309

310 For corn bran:

311  $Y_1 = 15.79 + 1.09X_2 + 2.86X_3 - 18.31X_4 - 0.04X_2X_3 + 0.89X_4^2$  (15)

312  $Y_2 = -281.05 + 6.28X_2 + 4.35X_3 + 8.81X_4 - 0.16eX_2X_4 - 0.03X_2^2 - 0.09X_3^2$  (16)

313

314 For pine sawdust:

315  $Y_1 = -0.66 + 0.06X_2 - 0.19X_3 - 2.34 \times 10^{-3} X_2X_3 + 0.01X_3^2$  (17)

316  $Y_2 = 1.47 + 0.27X_2 + 0.43X_3 - 3.80X_4 + 0.14X_4^2$  (18)

317

318 where  $Y_1$  and  $Y_2$  are G and RS responses respectively, and  $X_1$ ,  $X_2$ ,  $X_3$  and  $X_4$  are the  
 319 factors Ti, Te, A and AF, respectively. Only the factors that are significant for each  
 320 response have been included in the above equations.

321 Nevertheless, some statistical results were not satisfactory: the  $R^2$  obtained for  
 322 response G were 0.648, 0.742 and 0.699 for wheat bran, corn bran and pine sawdust,  
 323 respectively, implying that these models could explain only about 70 % of the variability  
 324 in the responses, with the remaining 30 % explained by the residue. Moreover, the  $p$   
 325 values corresponding to the lack of fit were all less than  $1 \times 10^{-4}$ , indicating that the  
 326 models are not suitable for prediction purposes.

327 In the case of the RS response, the  $R^2$  obtained were 0.964, 0.852 and 0.898 for  
 328 wheat bran, corn bran and pine sawdust, respectively. These values indicated that the  
 329 models could fit satisfactorily the responses. However, in the case of pine sawdust, the  $p$   
 330 value for the lack of fit was 0.022, once again meaning that the model could not be used

331 to perform predictions. In the remaining cases of wheat and corn bran, the lack of fit  
332 tests were not significant. These two models could fit the responses and could be used  
333 to perform further predictions.

334 Although some of the models cannot be used for prediction, an analysis of factor  
335 effects can be made. In most cases, when the individual contributions of Te, A and AF  
336 exerted positive or negative effects in a response, their interactions and/or quadratic  
337 contributions affected inversely the response, i.e.: exerted a negative effect or a positive  
338 effect, respectively. This indicates that the optimum factor values may be included in  
339 the tested ranges. With respect to the factor Ti, which was only evaluated in the case of  
340 wheat bran, two of its interactions (with AF in the G response and with A in the RS  
341 response) influence negatively the responses. According to these results, it is evident  
342 that these four factors exert a synergic effect on the hydrolysis processes.

343 It has been extensively described that these factors show a positive influence in  
344 sugar concentrations up to a certain extent, beyond which the inverse effect is observed  
345 [44–46]. Temperature is expected to have a positive effect, since it favors the rupture of  
346 heterocyclic ether bonds in the polysaccharides caused by protons, but up to a certain  
347 point, beyond which a negative effect can be observed [45,47]. Vieira Cannettieri et al.  
348 [43], working on *Eucalyptus grandis* wood, found that the time and temperature of  
349 hydrolysis have a negative effect on sugar yields due to its chemical degradation. Bower  
350 et al. [48] also found that an interaction between temperature and acid concentration  
351 exerted a negative effect on sugar yields, what could be explained, again, by sugars  
352 degradation to furfural and 5-hydroxymethylfurfural, mainly [44]. The behaviour of  
353 responses regarding A and AF can be explained taking into account that at high acid  
354 concentrations, the speed at which sugars degrade to furanes increases to the extent that

355 it can be 10-times the speed at which polisaccharides depolymerize, especially for  
356 hemicelluloses, producing the depletion of sugars yield [49].

357

#### 358 *4.2. Analysis by artificial neural networks*

359 Because the models obtained by means of QLS were not satisfactory, we resorted to  
360 the application of artificial neural networks based on the use of radial basis functions.

361 The values predicted by the RBF vs. the actual ones were employed to calculate the  $R^2$   
362 for both responses in the three hydrolysis process under study. The  $R^2$  values obtained  
363 for G response were 1.000, 1.000 and 0.995, and for RS response they were 0.979,

364 0.859 and 0.992 for wheat bran, corn bran and pine sawdust, respectively. These values  
365 indicate that the models obtained by means of RBF show improved fitting, mainly for G

366 response: 54.3 %, 34.77 % and 42.34 % for wheat bran, corn bran and pine sawdust,

367 respectively. This better performance of RBF may be attributed to its ability to

368 universally approximate non-linear systems. On the contrary, as was commented above,

369 QLS is restricted to only second-order polynomial models [21].

370 The first step in the RBF modeling of the design data was the estimation of the

371 optimal working RBF parameters, as well as the number of hidden neurons. This latter

372 number was tuned using one of the procedures included in Orr's RBF package, i.e.,

373 forward selection combined with regularization, which were briefly commented in

374 section 3.1. The criterion for stopping the addition of new basis functions was the

375 obtainment of a minimum in the so-called generalized cross-validation error, as defined

376 by Orr [ref. 40], which penalizes the mean squared error if an excessive number of

377 parameters is employed. Once the number of hidden neurons was set: a) wheat bran: 20

378 for glucose and 19 for reducing sugars, b) corn bran: 8 for glucose and 9 for reducing

379 sugars, c) pine sawdust: 8 for glucose and 15 for reducing sugars, straightforward RBF



380 analysis provided the values of the optimal working parameters, i.e., the centers, radii  
381 and weights which are quoted in Supplementary material.

382 Table 4 shows a comparison between the  $R^2$  values obtained by applying QLS and  
383 RBF, respectively. The improvement in model fitting for the wheat bran case can be  
384 seen in **Figure 2A and B**, which show the correlation between actual and predicted  
385 values for the responses using both models.

386 After modeling, the RBF parameters were used to find the optimal hydrolysis  
387 conditions by applying a methodology based on PSO. For the optimization process, a  
388 number of particles was set for each of the optimized systems, i.e., 15 particles for  
389 wheat bran and pine sawdust and 10 particles for corn bran. This appeared to be enough  
390 to cover the experimental factor space. Also, 15 generations were employed to find the  
391 optimal points in the multidimensional space for all the cases under study. These  
392 parameters (number of particles and generations) were assessed **by try and error**, in such  
393 a way that the convergence tolerance for the optimal values of the studied factors was  
394 less than 0.01%, i.e. that the difference between successive factor values after the  
395 generation cycle was less than 0.01%.

396 In comparison with other potential optimizing tools, such as exhaustive grid-search  
397 methods or genetic algorithms, PSO provides a reliable and fast manner of estimating  
398 the values of continuous experimental factors for optimizing the desirability function.

399 Table 4 shows the criteria employed to perform the optimization. Figure 3 shows the  
400 evolution of  $D$  as a function of the number of generations in the case of wheat bran.

401 For wheat bran hydrolysis, the optimal value found for  $D$  was 0.942, which  
402 corresponds to the following combination of factors:  $T_i$  59.6 min,  $T_e$  99.2 °C,  $A$  10.4%  
403 m/m and  $AF$  6.0 mLg<sup>-1</sup>. The response values that correspond to this combination were:  
404 54.8 gL<sup>-1</sup>  $G$  (individual desirability value  $d_G = 0.994$ ) and 108.2 gL<sup>-1</sup>  $RS$  ( $d_{RS} = 0.892$ ).

405 With respect to corn bran, the optimal combination was: Te 80.4 °C, A 20.5 % m/m and  
406 AF 4.2 mLg<sup>-1</sup> which corresponded to D = 1.000, 45.8 gL<sup>-1</sup> G (d<sub>G</sub> = 1.000) and 97.5 gL<sup>-1</sup>  
407 RS (d<sub>RS</sub> = 1.000). Finally, for pine sawdust, the optimal combination was: Te 80.2 °C, A  
408 36.8 % m/m and AF 9.0 mLg<sup>-1</sup>, which corresponds to D = 0.900. The predicted  
409 responses values were: 3.8 gL<sup>-1</sup> G (d<sub>G</sub> = 0.996) and 19.5 gL<sup>-1</sup> (d<sub>RS</sub> = 0.811). All these  
410 results were validated employing multiple layer perceptrons based ANN (data not  
411 shown). **Figure 4A and B** show the response surface for D as a function of Ti and Te,  
412 and as a function of A and AF, respectively, for wheat bran case, both at optimal values  
413 of the other factors.

414 An interesting observation can be made from the results obtained: there is some  
415 agreement with the optima reached by the application of experimental design followed  
416 of ANN-PSO and the highest experimental obtained values (see trials number 7, 18 and  
417 14, respectively, of **Table 1 and 2**). Nevertheless, this result is not common in the field  
418 of optimization, because most of the times in which the desirability function is applied,  
419 the optimal combination of factors do not necessarily match the best experiment. An  
420 erroneous conclusion could be extracted: the modeling is not necessary to get the  
421 optima. However, it must be strongly stated that modeling is the only way to know that  
422 there is agreement between trials maxima (corresponding to the design) and maxima  
423 reached by the modeling.

424 In sum, the RBF-PSO approach was capable of improving the model fitness in  
425 comparison to what was obtained by applying QLS, mainly for G responses. In addition,  
426 the values of D, which were all near 1, are indicative that the factors and responses have  
427 simultaneously desirable values. Consequently, it can be concluded that the application  
428 of the RBF-PSO approach allows to obtain more reliable results in comparison with  
429 classical QLS analysis.

430 Although the three studied raw materials have the same components, the optimal  
431 combinations predicted for each of them are specific for each material. This observation  
432 may be explained taking into account the specific macromolecular structure of the  
433 studied feedstocks: the arrangement of cellulose, lignin and hemicelluloses may vary  
434 among the different raw biomass. Then, different biomasses, subjected to hydrolysis  
435 reactions, may lead to different results. Additionally, almost all the optimal values were  
436 not at the edges of the tested factor ranges, which were adequately chosen, in order to  
437 find the optimal hydrolysis conditions.

438

## 439 **5. Conclusion**

440 The application of QLS was not capable of fitting adequate models that could  
441 satisfactorily explain the variability, mainly in G responses. On the contrary, RBF  
442 allowed obtaining more reliable models, a fact that can be attributed to its ability  
443 to approximate non-linear systems, whereas QLS is only capable of fitting second-order  
444 polynomial models with a reasonable number of experiments.

445 Moreover, with the introduction of a PSO approach, the optimal combinations that  
446 guarantee the maximization of the responses in the chemical hydrolysis processes of  
447 three different feedstocks were obtained. Thus, the RBF-PSO approach performed better  
448 than QLS in this particular study.

449 Finally, different biomass subjected to hydrolysis may lead to very different results  
450 due to its different macromolecular structure.

451

## 452 **Acknowledgments**

453           The authors are grateful to Universidad Nacional del Litoral (Project CAI+D N°  
454 12-65 and CAI+D 2009 Tipo III R2), to CONICET (Consejo Nacional de  
455 Investigaciones Científicas y Técnicas, Project PIP 2988) and to ANPCyT (Agencia  
456 Nacional de Científica y la Tecnológica, Project PICT 2010-0084) for financial support,  
457 and Arturo Simonetta for sharing his milling equipment. P.C.G. thanks CONICET for  
458 his fellowship.

459

## 460 **References**

461

- [1] Myers RH, Montgomery DC, Response Surface Methodology: Process and Product Optimization Using Designed Experiments (Wiley Series in Probability and Statistics), Wiley, New York; 2009.
- [2] Shi X-Y, Jin D-W, Sun Q-Y, Li W-W. Optimization of conditions for hydrogen production from brewery wastewater by anaerobic sludge using desirability function approach, *Renew. Energ.* 2010; 35:1493–1498.
- [3] Foudjo BUS, Kansci G, Fokou E, Lazar IM, Pontalier P-Y, Etoa F-X. Multi-response optimization of aqueous oil extraction from five varieties of cameroon-grown avocados. *Environ. Eng. Manag. J.* 2012; 11:2257–2263.
- [4] Gadhe A, Sonawane SS, Varma MN. Optimization of conditions for hydrogen production from complex dairy wastewater by anaerobic sludge using desirability function approach. *Int. J. Prod. Hydrogen* 2013; 38:6607–6617.
- [5] Dopar M, Kusic H, Koprivanac N. Treatment of simulated industrial wastewater by photo-Fenton process. Part I: The optimization of process parameters using design of experiments (DOE). *Chem. Engin. J.* 2011; 173: 267–279.

- [6] Kılıç M, Uzun BB, Pütün E, Pütün AE. Optimization of biodiesel production from castor oil using factorial design. *Fuel Process. Technol.*, 2013; 111: 105–110.
- [7] Severini C, Baiano A, De Pilli T, Romaniello R, Derossi A, Lebensm A, Prevention of enzymatic browning in sliced potatoes by blanching in boiling saline solutions. *Wiss Technol* 2003;36: 657-665.
- [8] Nardi JV, Acchar W, Hotza D. Enhancing the properties of ceramic products through mixture design and response surface analysis. *J Eur Ceramic Soc* 2004;24: 375-379.
- [9] Abnisa F, Wan Daud WMA, Sahu JN. Optimization and characterization studies on bio-oil production from palm shell by pyrolysis using response surface methodology. *Biomass Bioenergy* 2011;35: 3604-3616.
- [10] Lee KM, Gilmore DF. Formulation and process modelling of biopolymer (polyhydroxyalkanoates: PHAs) production from industrial wastes by novel crossed experimental design. *Process Biochem* 2005;40: 229-246.
- [11] Giordano PC, Martínez HD, Iglesias AA, Beccaria AJ, Goicoechea HC. Application of response surface methodology and artificial neural networks for optimization of recombinant *Oryza sativa* non-symbiotic hemoglobin 1 production by *Escherichia coli* in medium containing byproduct glycerol. *Bioresour. Technol.* 2010; 101:7537–7544.
- [12] Demain A, Davies J. *Manual of industrial microbiology and biotechnology*. Second Edition Washington: Am Soc Microbiol; 1999.
- [13] Zhi W, Song J, Ouyang F. Application of response surface methodology to the modeling of  $\alpha$ -amylase purification by aqueous two-phase systems. *J Biotechnol* 2005;118: 157-165.

- [14] Liu R-S, Tang Y-J. Tuber melanosporum fermentation medium optimization by Plackett–Burman design coupled with Draper–Lin small composite design and desirability function. *Biores. Technol.* 2010; 101:3139–3146.
- [15] Lim S, Le K-T. Optimization of supercritical methanol reactive extraction by Response Surface Methodology and product characterization from *Jatropha curcas* L. seeds. *Biores Technol*, 2013; 142:121–130.
- [16] Contesini FJ, Ibarguren C, Ferreira Grosso CR, de Oliveira Carvalho P, Harumi Sato H. Immobilization of glucosyltransferase from *Erwinia* sp. using two different techniques. *J Biotechnol*, 2012; 158:137–143.
- [17] Sella SRBR, Masetti C, Figueiredo LFM, Vandenberghe LPS, Minozzo JC, Soccol CR. Soybean molasses-based bioindicator system for monitoring sterilization process: Designing and performance evaluation. *Biotechnol Bioproc Eng* 2013; 18: 75–87.
- [18] Braga ARC, Gomes PA, Kalil SJ. Formulation of Culture Medium with Agroindustrial Waste for  $\beta$ -Galactosidase Production from *Kluyveromyces marxianus* ATCC 16045. *Food Bioproc Technol* 2012; 5: 1653–1663.
- [19] Larentis AL, Quintal Nicolau JFM, Argondizzo APC, Galler R, Rodrigues MI, Medeiros MA. Optimization of medium formulation and seed conditions for expression of mature PsaA (pneumococcal surface adhesin A) in *Escherichia coli* using a sequential experimental design strategy and response surface methodology. *J Ind Microbiol Biotechnol* 2012; 39: 897–908.
- [20] Liu YT, Long CN, Xuan SX, Lin BK, Long MN, Hu Z. Evaluation of culture conditions for cellulase production by two *Penicillium decumbens* under liquid fermentation conditions. *J Biotechnol* 2008;136: S328.
- [21] Desai KM, Survase SA, Saudagar PS, Lele SS, Singhal RS. Comparison of artificial neural network (ANN) and response surface methodology (RSM) in

fermentation media optimization: Case study of fermentative production of scleroglucan. *Biochem Eng J* 2008;41: 266–273.

[22] Leonardi D, Lamas MC, Salomón CJ, Olivieri AC. Development of novel formulations for Chagas' disease. Optimization of benznidazol chitosan microparticles based on artificial neural networks. *Int J Pharm* 2009;367: 140–147.

[23] Cheng S, Song Q, Wei D, Gao B. High-level production penicillin G acylase from *Alcaligenes faecalis* in recombinant *Escherichia coli* with optimization of carbon sources. *Enzyme Microb Technol* 2007;41: 326–330.

[24] Didier C, Forno G, Etcheverrigaray M, Kratjie R, Goicoechea, HC. Novel chemometric strategy based on the application of artificial neural networks to crossed-mixture design for the improvement of recombinant protein production in continuous culture. *Anal Chim Acta* 2009;650: 167-174.

[25] Giordano PC, Martínez HD, Iglesias AA, Beccaria AJ, Goicoechea HC. Application of response surface methodology and artificial neural networks for optimization of recombinant *Oriza sativa* non-symbiotic hemoglobin 1 production by *Escherichia coli* in medium containing byproduct glycerol. *Bioresour Technol* 2010;101: 7537-7544.

[26] Moreira GA, Micheloud GA, Beccaria AJ, Goicoechea HC. Optimization of the *Bacillus thuringiensis* var. kurstaki HD-1  $\delta$ -endotoxins production by using experimental mixture design and artificial neural networks. *Biochem Eng J* 2007;35: 48–55.

[27] Günay ME, Nikerel IE, Oner ET, Kirdar B, Yildirim R. Simultaneous modeling of enzyme production and biomass growth in recombinant *Escherichia coli* using artificial neural networks. *Biochem Eng J* 2007;42: 329–335.

- [28] Haykin S. Neural networks. A comprehensive foundation. Second edition Upper Saddle River, NJ: Prentice-Hall; 1999.
- [29] Derks EPPA, Sanchez Pastor MS, Buydens LMC. Robustness analysis of radial base function and multilayered feedforward neural network models. Chemom Intell Lab Syst 1995;28: 49-60.
- [30] Fidêncio PH, Poppi RJ, de Andrade JC. Determination of organic matter in soils using radial basis function networks and near infrared spectroscopy. Anal Chim Acta 2002;453: 125-134.
- [31] Fischbacher C, Jagemann KU, Danzer K, Muller UA, Papenkordt L, Schuler J. Enhancing calibration models for non-invasive near-infrared spectroscopical blood glucose determination. Fresenius J Anal Chem 1997;359: 78-82.
- [32] Carlin M, Kavli T, Lillekjendlie B. A comparison of four methods for non-linear data modelling. Chemom Intell Lab Syst 1994;23: 163-177.
- [33] Prakash O, Mehrotra S, Krishna A, Mishra BN. A neural network approach for the prediction of in vitro culture parameters for maximum biomass yields in hairy root cultures. J Theor Biol 2010;265: 579-585.
- [34] Kennedy J, Eberhart RC. Particle swarm optimization. In: Proc IEEE Int Conf Neural Networks, Perth, Australia, 1995, pp. 1942-1948.
- [35] Clerc M, Kennedy J. The Particle Swarm-Explosion, Stability, and Convergence in a Multidimensional Complex Space. IEEE Trans Evol Comput 2002;6: 58-73.
- [36] Liu L, Sun J, Zhang D, Du G, Chen J, Xu W. Culture conditions optimization of hyaluronic acid production by *Streptococcus zooepidemicus* based on radial basis function neural network and quantum-behaved particle swarm optimization algorithm. Enz Mic Tec 2009;44: 24-32.



- [37] Kitayama S, Yasuda K, Yamazaki K. Integrative optimization by RBF network and particle swarm optimization. *Elec Com Japan* 2009;92: 31-42.
- [38] Derringer G, Suich R. Simultaneous optimization of several response variables, *J Qual Technol* 1980;12: 214-219.
- [39] Miller GL. Use of dinitrosalicylic acid reagent for determination of reducing sugar. *Anal Chem* 1959;31: 426-428.
- [40] Orr MJL. Matlab functions for radial basis function networks. Technical report. Institute for Adaptive and Neural Computation, Division of Informatics, Edinburgh University; 1999.
- [41] Orr MJL. Regularisation in the selection of radial basis function centres. *Neural Comp* 1995;7: 606-623.
- [42] Giordano PC, Beccara AJ, Goicoechea HC. Significant factors selection in the chemical and enzymatic hydrolysis of lignocellulosic residues by a genetic algorithm analysis and comparison with the standard Plackett-Burman methodology. *Bioresour Technol* 2011;102: 10602-10610.
- [43] Vieira Canettieri E, Jackson de Moraes Rocha G, Andrade de Carvalho Jr. J, Batista de Almeida e Silva J. Optimization of acid hydrolysis from the hemicellulosic fraction of *Eucalyptus grandis* residue using response surface methodology. *Bioresour Technol* 2007;98: 422-428.
- [44] Choteborska P, Palmarola-Adrados B, Galbe M, Zacchi G, Melzoch K, Rychtera M. Processing of wheat bran to sugar solution. *J Food Eng* 2004;61: 561–565.
- [45] Aguilar R, Ramirez JA, Garrote J, Vazquez M. Kinetic study of the acid hydrolysis of sugar cane bagasse. *J Food Eng* 2002;55: 309–318.

[46] ] Iranmahboob J, Nadim F, Monemi S. Optimizing acid-hydrolysis: a critical step for production of ethanol from mixed wood chips. *Biomass Bioenergy* 2002;22: 401–404.

[47] Yoo CG, Lee CW, Kim TH. Optimization of two-stage fractionation process for lignocellulosic biomass using response surface methodology (RSM). *Biomass Bioenergy* 2011;35: 4901-4909.

[48] Bower S, Wickramasinghe R, Nagle NJ, Schell DJ. Modeling sucrose hydrolysis in dilute sulfuric acid solutions at pretreatment conditions for lignocellulosic biomass. *Bioresour Technol* 2008;99: 7354-7362.

[49] Sanchez G, Pilcher L, Roslander C, Modig T, Galbe M, Liden G. Dilute-acid hydrolysis for fermentation of the Bolivian straw material Paja Brava. *Bioresour Technol* 2004;93: 249–256.



462 **Figure captions**

463

464 **Fig. 1.** Optimization flowchart by using particle swarm optimization.

465

466 **Fig. 2.** Correlation between actual and predicted values for responses glucose (A) and  
467 reducing sugars (B), fitted applying quadratic least-squares fit methodology and  
468 artificial neural networks based in radial basis functions, for wheat bran.

469

470 **Fig. 3.** Evolution of the global desirability function (D) as a function of the number of  
471 generations when applying radial basis functions and particle swarm optimization in  
472 the case of wheat bran.

473

474 **Fig. 4.** (A) Response surface for the desirability as a function of time of hydrolysis  
475 (minutes), temperature of hydrolysis (°C). (B) Response surface for the desirability as a  
476 function of sulphuric acid concentration (% m/m) and acid solution/feedstock ratio (g  
477 acid sol/g residue). Both figures at optimal values of the other factors and for wheat  
478 bran case.

**Table 1** Central composite design built to find the optimal conditions of the chemical

Experiment	Factors <sup>a</sup>			Responses <sup>b</sup>			
	Te	A	AF	G		RS	
				CB	PS	CB	PS
1	100.0	10.0	12.0	26.9	1.6	56.7	8.9
2	80.0	20.0	9.0	0.0	0.3	70.3	8.3
3	113.6	20.0	9.0	0.0	0.1	54.2	16.4
4	80.0	20.0	9.0	0.1	0.2	74.0	8.4
5	46.4	20.0	9.0	0.0	0.2	10.7	2.6
6	80.0	20.0	9.0	0.1	0.0	65.9	8.8
7	60.0	30.0	12.0	0.0	0.1	49.8	3.2
8	100.0	10.0	6.0	41.1	3.0	95.5	19.5
9	80.0	20.0	9.0	0.0	0.1	73.3	8.3
10	100.0	30.0	6.0	0.0	0.0	91.6	23.7
11	80.0	3.2	9.0	1.3	2.4	19.0	2.6
12	60.0	30.0	6.0	0.2	0.1	52.0	13.4
13	80.0	20.0	14.1	0.0	0.7	48.8	3.8
14	80.0	40.0	9.0	0.3	3.6	50.9	19.4
15	100.0	30.0	12.0	0.0	0.2	53.0	18.5
16	80.0	20.0	9.0	0.0	0.5	69.1	5.8
17	60.0	10.0	12.0	0.0	0.5	34.2	1.25
18	80.0	20.0	3.9	45.4	0.2	97.2	18.8
19	80.0	20.0	9.0	0.2	0.2	55.1	6.9
20	60.0	10.0	6.0	0.6	0.4	33.2	1.8

<sup>a</sup>Te (°C): temperature of hydrolysis, A (% m/m): sulphuric acid concentration, AF (g acid sol/g residue): acid solution/feedstock ratio.

<sup>b</sup>G (g L<sup>-1</sup>): concentration of glucose, RS (g L<sup>-1</sup>): concentration of reducing sugars, CB: corn bran, PS: pine sawdust.

hydrolysis of corn bran and pine sawdust.

**Table 2** Central composite design built to find the optimal conditions of the the chemical hydrolysis of wheat bran.

Experiment	Factors <sup>a</sup>				Responses <sup>b</sup>		Experiment	Factors <sup>a</sup>				Responses <sup>b</sup>	
	Ti	Te	A	AF	G	RS		Ti	Te	A	AF	G	RS
1	45.0	80.0	20.0	9.0	0.0	80.8	16	30.0	100.0	30.0	12.0	0.2	52.3
2	60.0	60.0	10.0	6.0	2.7	30.3	17	60.0	60.0	10.0	12.0	1.3	14.5
3	45.0	120.0	20.0	9.0	0.1	51.3	18	45.0	80.0	20.0	9.0	0.2	69.4
4	75.0	80.0	20.0	9.0	0.0	80.4	19	30.0	100.0	30.0	6.0	0.2	91.1
5	45.0	80.0	20.0	9.0	0.1	76.1	20	60.0	60.0	30.0	12.0	0.0	52.0
6	45.0	80.0	40.0	9.0	0.4	52.3	21	30.0	60.0	10.0	12.0	1.4	6.3
7	60.0	100.0	10.0	6.0	55.1	106.8	22	30.0	100.0	10.0	12.0	26.9	48.6
8	60.0	100.0	30.0	12.0	0.1	46.4	23	45.0	80.0	20.0	3.0	52.6	117.4
9	45.0	80.0	20.0	15.0	0.0	54.4	24	60.0	100.0	30.0	6.0	0.2	77.9
10	45.0	80.0	20.0	9.0	0.0	69.0	25	60.0	60.0	30.0	6.0	21.0	50.1
11	30.0	60.0	30.0	12.0	0.2	51.0	26	45.0	40.0	20.0	9.0	1.2	10.3
12	45.0	80.0	20.0	9.0	0.0	76.5	27	30.0	100.0	10.0	6.0	0.2	84.1
13	45.0	80.0	20.0	9.0	0.1	78.1	28	30.0	60.0	30.0	6.0	0.3	79.8
14	15.0	80.0	20.0	9.0	0.1	67.5	29	30.0	60.0	10.0	6.0	1.8	13.9
15	45.0	80.0	0.0	9.0	0.7	3.7	30	60.0	100.0	10.0	12.0	27.8	56.6

<sup>a</sup>Ti (minutes): time of hydrolysis, Te (°C): temperature of hydrolysis, A (% m/m): sulphuric acid concentration, AF (g acid sol/g residue): acid solution/feedstock ratio.

<sup>b</sup>G (g L<sup>-1</sup>): concentration of glucose, RS (g L<sup>-1</sup>): concentration of reducing sugars

**Table 3** Statistics obtained by means of QLS and RBF

Feedstock		Wheat bran		Corn bran		Pine Sawdust	
Response <sup>a</sup>		G	RS	G	RS	G	RS
QLS <sup>b</sup>	Model	Quadratic ( <i>p</i> =0.0007)	Quadratic ( <i>p</i> <0.0001)	Quadratic ( <i>p</i> =0.0009)	Quadratic ( <i>p</i> <0.0001)	Quadratic ( <i>p</i> =0.0114)	Quadratic ( <i>p</i> <0.0001)
	Lack of fit	Significant ( <i>p</i> <0.0001)	Not significant ( <i>p</i> =0.1833)	Significant ( <i>p</i> <0.0001)	Not significant ( <i>p</i> =0.1063)	Significant ( <i>p</i> =0.0021)	Significant ( <i>p</i> =0.0219)
	<i>R</i> <sup>2</sup>	0.648	0.964	0.742	0.852	0.699	0.898
RBF <sup>c</sup>	<i>R</i> <sup>2</sup>	1.000	0.979	1.000	0.859	0.995	0.992

<sup>a</sup>G: concentration of glucose; RS: concentration of reducing sugars.

<sup>b</sup>QLS: quadratic least-squares fit methodology

<sup>c</sup>RBF: artificial neural networks based in radial basis functions.

**Table 4** Criteria used for the optimization of multiple responses.

Factors <sup>a</sup> and responses <sup>b</sup>	Optimization criteria	Lower limit <sup>c</sup>			Upper limit <sup>c</sup>		
		WB	CB	PS	WB <sup>c</sup>	CB	PS
Ti (min)	In range	15.0	–	–	75.0	–	–
Te (°C)	In range	40.0	46.4	46.4	120.0	113.6	113.6
A (% m/m)	In range	0.0	3.2	3.2	40.0	36.8	36.8
AF (mLg <sup>-1</sup> )	In range	3.0	3.9	3.9	15.0	14.1	14.1
G (gL <sup>-1</sup> )	Maximize	0.0	0.0	0.0	55.1	45.4	3.6
RS (gL <sup>-1</sup> )	Maximize	3.7	10.7	2.6	117.4	97.2	23.7

<sup>a</sup>Ti: time of hydrolysis. Te: temperature of hydrolysis. A: concentration of sulphuric acid. AF: acid solution/feedstock ratio.

<sup>b</sup>G: concentration of glucose. RS: concentration of reducing sugars.

<sup>c</sup>WB: wheat bran, CB: corn bran, PS: pine sawdust.